RSC Advances

PAPER

View Article Online
View Journal | View Issue

Cite this: *RSC Adv.*, 2018, **8**, 11316

Role of NH_4 ions in successive phase transitions of perovskite type $(NH_4)_2ZnX_4$ (X = Cl, Br) by ^1H MAS NMR and ^{14}N NMR

Ae Ran Lim *[ab]

Received 10th February 2018
Accepted 12th March 2018

DOI: 10.1039/c8ra01315b

rsc.li/rsc-advances

The ^1H chemical shifts and the spin-lattice relaxation time, $T_{1\rho}$, in the rotating frame of $(NH_4)_2ZnX_4$ (X = Cl, Br) are observed in order to investigate local phenomena related to successive phase transitions. The temperature dependence of $T_{1\rho}$ values for ^1H showed a minimum, and the $T_{1\rho}$ values for ^1H appeared to be governed by tumbling molecular motions at high temperatures. In addition, ^{14}N NMR spectra are studied in each phase of $(NH_4)_2ZnX_4$ single crystals in the laboratory frame. The phase transition temperatures strongly affect the ^{14}N number of symmetry related nitrogen centers within the unit cell. The ^1H MAS NMR and ^{14}N NMR results are discussed to elucidate the roles of NH_4 ions during the phase transitions of $(NH_4)_2ZnX_4$.

1. Introduction

Perovskite A_2BX_4 type (A = NH_4, K, Rb, Cs; B = Zn, Co, Cu, Fe, Zn, Cd; X = Cl, Br) crystals have received a great deal of attention because of their nonlinear optical properties, and also because of the significant diversity of their structural phase transitions.[1–10] The prototype of the crystal structures of this family is that of β-K_2SO_4, which consists of isolated BX_4^{2-} tetrahedra and monovalent A^+ cations placed in two inequivalent cavities. Ammonium tetrachlorozincate, $(NH_4)_2ZnCl_4$, and ammonium tetrabromozincate, $(NH_4)_2ZnBr_4$, belong to the family of crystals of the perovskite A_2BX_4 type and are known to undergo several phase transitions. Although the physical properties of $(NH_4)_2ZnCl_4$ and $(NH_4)_2ZnBr_4$ have been studied by several research groups, the structural geometry changes during the phase transitions of the two compounds have not been fully understood. Here, the phase transition temperatures and dynamics of the cations in $(NH_4)_2ZnCl_4$ and $(NH_4)_2ZnBr_4$ are important. The potential applications of these materials are strongly affected by the phase transitions and dynamics of the cations.[11]

$(NH_4)_2ZnCl_4$ undergoes five phase transitions: those between phases I and II at 406 K ($=T_{C1}$) and phases II and III at 364 K ($=T_{C2}$) are well-known, and the successive phase transitions at 319 K ($=T_{C3}$), 271 K ($=T_{C4}$), and 266 K ($=T_{C5}$) have also been reported;[12–14] the phases involved in these transitions are denoted by VI, V, IV, III, II, and I in order of increasing temperature, as shown in Table 1. The structure of $(NH_4)_2ZnCl_4$ in the normal phase, phase I (above 406 K), is orthorhombic with a_o = 9.274 Å, b_o = 12.620 Å, and c_o = 7.211 Å, and space group *Pnma*.[12] Upon cooling, there is a phase transition at 406 K to an incommensurate phase that is stable down to 364 K.[15] The structure in phase III between 364 K and 319 K is orthorhombic with $a = a_o$, $b = b_o$, $c = 4c_o$, and the space group $Pn2_1a$.[12,16,17] The room temperature phase, phase IV, is antiferroelectric with a pseudo-orthorhombic monoclinic structure and space group *Pa*.[12] The region between 271 K and 266 K is mixed phase.[14] Below 266 K, the lattice is constant with an orthorhombic structure, where $a = a_o$, $b = b_o$, and $c = 3c_o$.[12,17]

On the other hand, the successive phase transitions of $(NH_4)_2ZnBr_4$ have been reported at 216 K ($=T_{C3}$), 395 K ($=T_{C2}$), and 432 K ($=T_{C1}$),[18–20] as shown in Table 1; the phases involved in these transitions are represented by IV, III, II, and I in order of increasing temperature. The structures of $(NH_4)_2ZnBr_4$ crystals in phases I, III, and IV are shown in Fig. 1. In phase I (above 432 K), the structure of $(NH_4)_2ZnBr_4$ is orthorhombic with a_o = 7.649 Å, b_o = 13.353 Å, c_o = 9.727 Å, and space group *Pmcn*.[21,22] Upon cooling, there is a phase transition at 432 K to an incommensurate phase II that is stable down to 395 K. The structure in phase III, between 395 K and 216 K, is monoclinic with $a = a_o$, $b = b_o$, $c = 4c_o$, $\beta = 90.00(3)^\circ$, and space group $P2_1/c11$.[22] The low-temperature phase IV is orthorhombic with $a = a_o$, $b = b_o$, $c = 3c_o$, and space group $P2_1cn$.[22]

The ^1H spin-lattice relaxation times of $(NH_4)_2ZnCl_4$ and $(NH_4)_2ZnBr_4$ crystals have been obtained in the laboratory frame by Lim *et al.*[23–25] and Ramesh *et al.*,[26] respectively. The molecular dynamics and phase transitions of $(NH_4)_2ZnCl_4$ single crystals were reported previously. There were two crystallographically inequivalent NH_4 sites, namely $NH_4(1)$ and $NH_4(2)$, in the $(NH_4)_2ZnCl_4$. The ^1H spin-lattice relaxation time T_1 in the laboratory frame was observed to vary continuously with temperature without jumps or changes. The ^1H T_1 passes

[a]*Analytical Laboratory of Advanced Ferroelectric Crystals, Jeonju University, Jeonju 55069, Korea. E-mail: aeranlim@hanmail.net; arlim@jj.ac.kr*
[b]*Department of Science Education, Jeonju University, Jeonju 55069, Korea*

Table 1 Phase transition temperatures, crystal structures, space groups, and lattice constants of $(NH_4)_2ZnX_4$ (X = Cl, Br)

$(NH_4)_2ZnCl_4$						
Transition temperature		T_{C5} (=266K)	T_{C4} (=271 K)	T_{C3} (=319 K)	T_{C2} (=364 K)	T_{C1} (=406 K)
Phase	VI	V	IV	III	II	I
Structure	Orthorhombic	Mixed phase	Monoclinic	Orthorhombic	Incommensurate	Orthorhombic
Space group	$Pna2_1$		Pa	$Pn2_1a$		$Pnma$
Lattice constant	$a = a_o$		$a = a_o$	$a = a_o$		$a_o = 9.274$ Å
	$b = b_o$		$b = b_o$	$b = b_o$		$b_o = 12.620$ Å
	$c = 3c_o$		$c = 4c_o$	$c = 4c_o$		$c_o = 7.211$ Å
			$\beta = 89.992°$			
	$Z = 12$	$Z = 12$, 14, 16	$Z = 16$	$Z = 16$		$Z = 4$
Reference	12 and 17	14	12	12, 16 and 17	15	12
$(NH_4)_2ZnBr_4$						
Transition temperature			T_{C3} (=216 K)	T_{C2} (=395 K)	T_{C1} (=432 K)	
Phase			IV	III	II	I
Structure			Orthorhombic	Monoclinic	Incommensurate	Orthorhombic
Space group			$P2_1cn$	$P2_1/c11$		$Pmcn$
Lattice constant			$a = a_o$	$a = a_o$		$a_o = 7.649$ Å
			$b = b_o$	$b = b_o$		$b_o = 13.353$ Å
			$c = 3c_o$	$c = 4c_o$		$c_o = 9.727$ Å
				$\beta = 90.00(3)°$		
			$Z = 12$	$Z = 16$		$Z = 4$
Reference			22	22	20	21 and 22

through a minimum value near 220 K; the presence of this minimum was attributed to the reorientation of the NH_4 groups. In addition, the ^{14}N nuclear magnetic resonance (NMR) results in phase I of $(NH_4)_2ZnCl_4$ were reported for the two inequivalent sites N(1) and N(2): the quadrupole coupling constant, e^2qQ/h, and asymmetry parameter, η, were $e^2qQ/h =$ 105.5 kHz and $\eta = 0.96$ for N(1), and $e^2qQ/h = 48.2$ kHz and $\eta =$ 0.087 for N(2).[27]

The NMR method enables the study of a lattice's local properties, and is particularly useful in those cases that require information on the behavior of individual structural groups. Measurements of $T_{1\rho}$ obtained by magic angle spinning (MAS) NMR in the rotating frame are advantageous in that they allow for probing of molecular motion in the kHz range, whereas T_1 values obtained by state NMR in a laboratory frame reflect motion in the MHz range.[28]

The aim of this paper is to clarify the structural changes associated with the successive phase transitions in $(NH_4)_2ZnX_4$ (X = Cl, Br). Detailed studies of the molecular motions are necessary in order to explain the mechanisms of the phase transitions of $(NH_4)_2ZnX_4$. The temperature dependences of the MAS NMR spectra and the spin-lattice relaxation times, $T_{1\rho}$, in the rotating frame for the ^1H nuclei in $(NH_4)_2ZnX_4$ were investigated using a pulsed NMR spectroscopy. In addition, the ^{14}N NMR spectra in $(NH_4)_2ZnX_4$ single crystals were obtained by static NMR in the laboratory frame, as a function of temperature. The ^1H MAS NMR and ^{14}N static NMR results were analyzed to elucidate the roles of NH_4 ions during the phase transitions of $(NH_4)_2ZnCl_4$ and $(NH_4)_2ZnBr_4$. The $T_{1\rho}$ values by ^1H MAS NMR obtained here and the previously reported T_1 values by ^1H static NMR are compared. In addition, the information regarding the structural geometry of nitrogen environments in NH_4^+ is discussed as a function of temperature.

2. Experimental method

Single crystals of $(NH_4)_2ZnCl_4$ and $(NH_4)_2ZnBr_4$ were obtained by the slow evaporation of aqueous solutions with the appropriate molar ratios of NH_4Cl and $ZnCl_2$, and NH_4Br and $ZnBr_2$, respectively, at 298 K.[12,29,30] These single crystals exhibited hexagonal shapes that were transparent and colorless.

^1H MAS NMR spectra and the spin-lattice relaxation times, $T_{1\rho}$, in the rotating frame in $(NH_4)_2ZnCl_4$ and $(NH_4)_2ZnBr_4$ were measured in a static magnetic field of 9.4 T and Larmor frequency of $\omega_0/2\pi = 400.13$ MHz, using a Bruker 400 MHz NMR spectroscopy at the Korea Basic Science Institute, Western Seoul Center. The chemical shifts were measured with respect to tetramethylsilane (TMS). Powder samples were placed inside a 4 mm cross-polarization (CP)/MAS probe, and the MAS rate was set to 5 kHz to minimize spinning sideband overlap. ^1H $T_{1\rho}$ values were determined using a $\pi/2$–t sequence by varying the duration of spin-locking pulses. The widths of the $\pi/2$ pulse used to measure the $T_{1\rho}$ values of ^1H in $(NH_4)_2ZnCl_4$ and $(NH_4)_2ZnBr_4$ were 4.35 μs and 3.7 μs, respectively, with the spin-locking field equaling 57.47 kHz and 67.56 kHz.

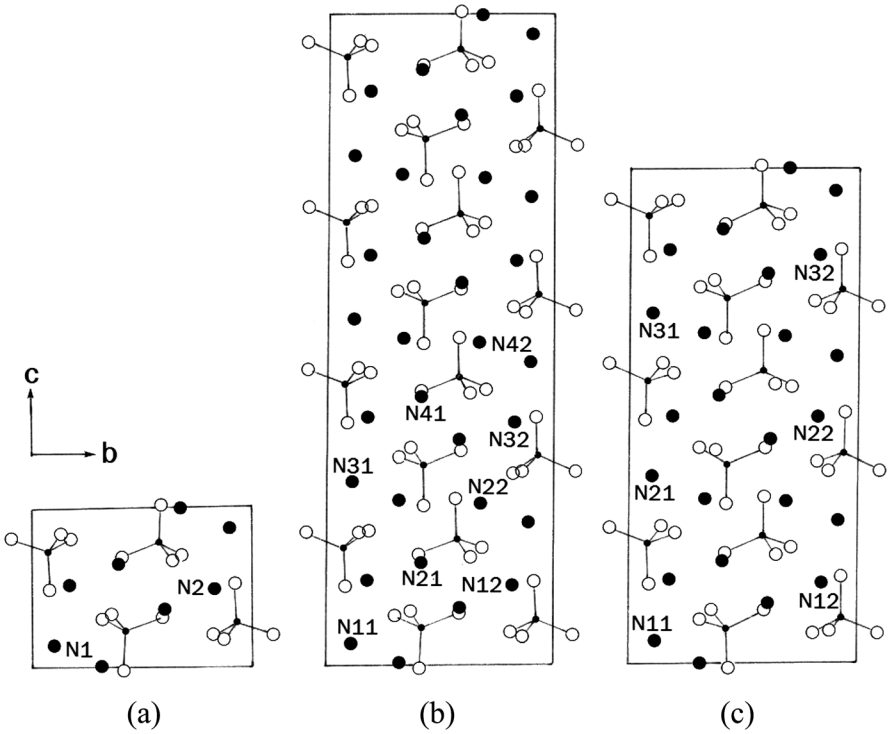

Fig. 1 Projection of the structure along the *a*-axis in phases (a) I, (b) III, and (c) IV of $(NH_4)_2ZnBr_4$ crystal.

In addition, the ^{14}N NMR spectra of the $(NH_4)_2ZnCl_4$ and $(NH_4)_2ZnBr_4$ single crystals in the laboratory frame were measured using a Unity INOVA 600 NMR spectroscopy at the Korea Basic Science Institute, Western Seoul Center. The static magnetic field was 14.1 T, and the Larmor frequency was set to $\omega_0/2\pi = 43.342$ MHz. The ^{14}N NMR experiments were performed using a solid echo sequence of $\pi/2$–t–$\pi/2$–t. The widths of the $\pi/2$ pulse for ^{14}N in $(NH_4)_2ZnCl_4$ and $(NH_4)_2ZnBr_4$ were 4 μs and 3.7 μs, respectively. The measurements of ^1H MAS NMR in the rotating frame and ^{14}N NMR in the laboratory frame were obtained over the temperature range of 180–430 K. Sample temperatures on MAS NMR and static NMR were held constant within ±0.5 K by controlling the helium gas flow and heater current.

3. Experimental results and discussion

3.1 Phase transition temperatures

The phase transition temperatures for $(NH_4)_2ZnCl_4$ and $(NH_4)_2ZnBr_4$ single crystals have not yet been accurately established, as shown in Fig. 2. Here, the small vertical bars were represented the phase transition temperatures reported by several groups. In the case of $(NH_4)_2ZnCl_4$, this crystal exhibits three temperature dependence anomalies in the dielectric, thermal, and X-ray diffraction measurements at 270 K, 319 K, and 406 K, respectively, as reported by Matsunaga *et al.*[13] Furthermore, anomalies characteristic of phase transitions reported by Agarwal *et al.*[31] have been found in the Raman spectra investigations at 194 K, 266 K, 271 K, 319 K, and 406 K. According to Gillet *et al.*,[32] the occurrence of phase transitions at 253 K, 256 K, 319 K, 364 K, and 406 K was also confirmed on the basis of the Brillouin investigation.[32] In addition, thermal expansion changes at temperatures of 253 K, 255 K, 323 K, 362 K, and 406 K were reported by Tylczynski *et al.*[29] In the case of $(NH_4)_2ZnBr_4$, phase transition temperatures have been reported at 216 K, 395 K, and 432 K by Osaka *et al.*,[18] and an additional phase transition at 365 K was reported by Moskalev *et al.*[15] in their investigation of a $(NH_4)_2ZnBr_4$ crystal using ^{81}Br nuclear quadrupole resonance (NQR), differential thermal analysis (DTA), and dielectric measurements. Fig. 2 shows that the phase transition temperatures obtained by several experiments are inconsistent for $(NH_4)_2ZnCl_4$ and $(NH_4)_2ZnBr_4$, respectively.

In order to determine the phase transition temperatures for the $(NH_4)_2ZnCl_4$ and $(NH_4)_2ZnBr_4$ single crystals obtained here, differential scanning calorimetry (DSC) measurements were taken with a DuPont 2010 DSC instrument at a heating rate of 10 °C min^{-1}. The DSC measurements revealed three endothermic peaks at 270 K, 320 K, and 406 K for $(NH_4)_2ZnCl_4$, and four endothermic peaks at 216 K, 362 K, 396 K, and 432 K for $(NH_4)_2ZnBr_4$, as shown in Fig. 3. These endothermic peaks were related to the phase transitions, and the temperatures were consistent with those previously reported by Matsunaga *et al.*[13] and Moskalev *et al.*[15] The phase transition temperatures of $(NH_4)_2ZnX_4$ may vary according to the conditions of crystal growth.

3.2 Molecular motion near phase transition temperatures from ^1H MAS NMR

The ^1H MAS NMR spectra in $(NH_4)_2ZnCl_4$ and $(NH_4)_2ZnBr_4$ were measured as a function of temperature. At room temperature, $(NH_4)_2ZnCl_4$ and $(NH_4)_2ZnBr_4$ showed only one peak each, at

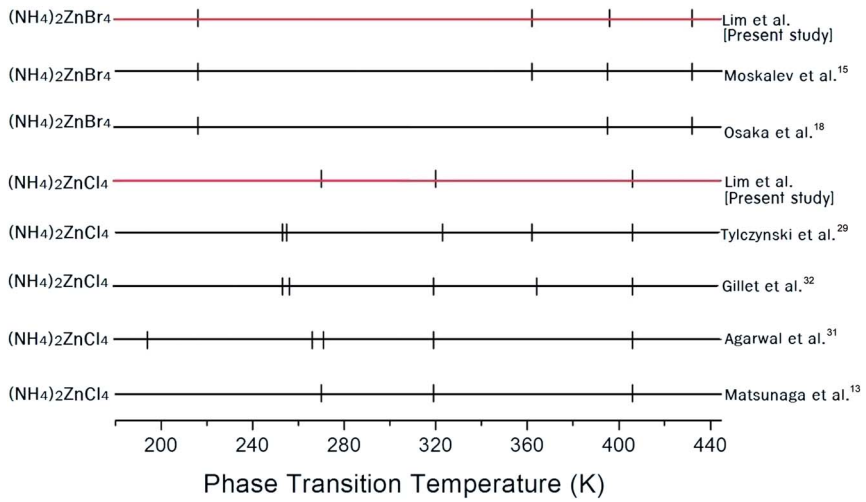

Fig. 2 Phase transition temperatures (K) for $(NH_4)_2ZnX_4$ (X = Cl, Br) reported by several groups.

chemical shifts of $\delta = 6.53$ ppm and $\delta = 6.66$ ppm, respectively, as shown in Fig. 4. The phase transition temperatures of $(NH_4)_2ZnCl_4$ are denoted by solid lines, and those of $(NH_4)_2ZnBr_4$ are denoted dash lines. The chemical shifts of the two materials did not change near the phase transition temperatures. The ^1H chemical shifts of $(NH_4)_2ZnCl_4$ decreased with increasing temperature, whereas the ^1H chemical shift of $(NH_4)_2ZnBr_4$ increased with increasing temperature. From the chemical shift for ^1H, the proton environments in N–H···Cl bond and the proton environments in N–H···Br bond were very different. This difference of chemical shifts was possibly due to the difference between the electron structures of halogen ions.

The decay traces for the ^1H resonance line in $(NH_4)_2ZnCl_4$ and $(NH_4)_2ZnBr_4$ are represented by a single exponential function of $M(t) = M(\infty)\exp(-t/T_{1\rho})$, where $M(t)$ is the magnetization as a function of the spin-locking pulse duration t, and $M(\infty)$ is the total nuclear magnetization of ^1H at thermal equilibrium.[14] The decay traces for the ^1H nuclei varied with the delay time, and these decay traces also varied depending upon the temperature. The decay traces fitted with the single exponential function for delay times. From the slopes of the decay traces, the ^1H spin-lattice relaxation times, $T_{1\rho}$, in the rotating frame for the $(NH_4)_2ZnCl_4$ and $(NH_4)_2ZnBr_4$ were obtained as a function of temperature, as shown in Fig. 5. The $T_{1\rho}$ values of ^1H were significantly different in the high-temperature and low-temperature regions. The significant difference in the $T_{1\rho}$ values indicates that $(NH_4)_2ZnCl_4$ and $(NH_4)_2ZnBr_4$ are strongly affected, which considered to be mainly the result of molecular motions. The ^1H $T_{1\rho}$ data showed no evidence of a change near the phase transition temperatures. The trend of ^1H $T_{1\rho}$ in $(NH_4)_2ZnCl_4$ resembled that of ^1H $T_{1\rho}$ in $(NH_4)_2ZnBr_4$. The two $T_{1\rho}$ series displayed similar trends, both decreasing quickly above 310 K. The variation of $T_{1\rho}$ with temperature exhibited a shallow minimum of 7.2 ms at 430 K in the case of $(NH_4)_2ZnBr_4$, indicating that distinct molecular motion is present. The $T_{1\rho}$ minimum is considered to be clearly attributable to the tumbling motion of NH_4^+ ions. The $T_{1\rho}$ values are related to the corresponding values of the rotational correlation time, τ_C,

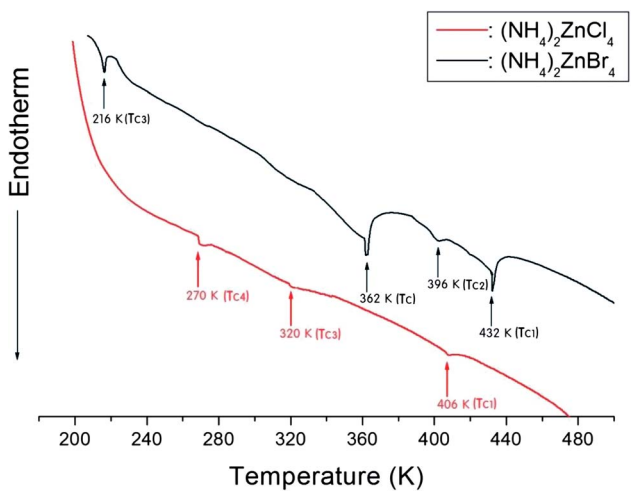

Fig. 3 Differential scanning calorimetry (DSC) thermograms of $(NH_4)_2ZnCl_4$ and $(NH_4)_2ZnBr_4$ single crystals.

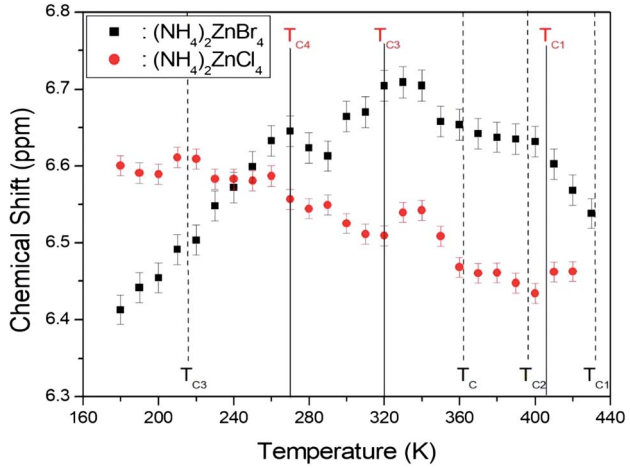

Fig. 4 Chemical shifts of ^1H MAS NMR spectra in $(NH_4)_2ZnCl_4$ and $(NH_4)_2ZnBr_4$ as a function of temperature ($(NH_4)_2ZnCl_4$: solid lines, $(NH_4)_2ZnBr_4$: dash lines).

which directly measures the rate of motion. The experimental $T_{1\rho}$ value can be expressed in terms of τ_C using molecular motion, as suggested by the Bloembergen–Purcell–Pound (BPP) theory.[33] The $T_{1\rho}$ value in the rotating frame can also be expressed in terms of τ_C using molecular motion.[28,34]

$$1/T_{1\rho} = (n/20)(\gamma_H\gamma_N\hbar/r_{H\text{–}N}{}^3)^2[4f(\omega_1) + f(\omega_H - \omega_N) + 3f(\omega_N) + 6f(\omega_H + \omega_N) + 6f(\omega_H)] \quad (1)$$

Here:

$$f(\omega_1) = \tau_C/[1 + \omega_1{}^2\tau_C{}^2]$$

$$f(\omega_H - \omega_N) = \tau_C/[1 + (\omega_H - \omega_N)^2\tau_C{}^2]$$

$$f(\omega_N) = \tau_C/[1 + \omega_N{}^2\tau_C{}^2]$$

$$f(\omega_H + \omega_N) = \tau_C/[1 + (\omega_H + \omega_N)^2\tau_C{}^2]$$

$$f(\omega_H) = \tau_C/[1 + \omega_H{}^2\tau_C{}^2]$$

In the equation, γ_H and γ_N are the gyromagnetic ratios for the ^{1}H and ^{14}N nuclei, respectively; n is the number of directly bound protons; $r_{H\text{–}N}$ is the H–N internuclear distance; $\hbar$ is the reduced Planck constant; ω_H and ω_N are the Larmor frequencies of ^{1}H and ^{14}N, respectively; and ω_1 is the spin-lock field frequency of 67.56 kHz. Here, the $f(\omega_1)$ is non-zero, *i.e.*, the τ_C is much less than the Larmor frequencies, therefore all of the other terms is far smaller than the $f(\omega_1)$ term. We analyzed our data by assuming that $T_{1\rho}$ would show a minimum when $\omega_1\tau_C = 1$, and that the relation between $T_{1\rho}$ and the characteristic frequency of motion, $1/\tau_C$, could be applied. The coefficient in eqn (1) can be determined because the $T_{1\rho}$ curve displays a minimum and because the value of τ_C can be obtained from $\omega_1\tau_C = 1$; thus, $(n/20)(\gamma_H\gamma_N\hbar/r_{H\text{–}N}{}^3)^2 \approx 4.66 \times 10^6$ in the BPP formula. We were then able to calculate the correlation time τ_C as a function of temperature. The temperature dependence of τ_C follows a simple Arrhenius expression:[34,35]

$$\tau_C = \tau_o \exp(-E_a/RT), \quad (2)$$

where τ_o is a pre-exponential factor, T is the temperature, R is the gas constant, and E_a is an activation energy. Thus, the slope of the linear portion of a semi-logarithmic plot should yield E_a. The value of E_a for the tumbling motion can be obtained from a plot of $\log \tau_C$ *versus* $1000/T$. We obtained $E_a = 36.69 \pm 0.66$ kJ mol^{-1} for the tumbling motion of ^{1}H in $(NH_4)_2ZnBr_4$ at high temperature. This value is very similar to that for ^{1}H in $(NH_4)_2ZnCl_4$, and is the same within the error range. And, the E_a for $(NH_4)_2ZnCl_4$ and $(NH_4)_2ZnBr_4$ at low temperature is 0.32 ± 0.30 kJ mol^{-1} and 2.25 ± 0.37 kJ mol^{-1}, respectively.

On the other hand, the ^{1}H spin-lattice relaxation time T_1 in the laboratory frame in $(NH_4)_2ZnCl_4$ previously reported was obtained as a function of temperature, as shown in Fig. 5.[23–25] In the high temperature region, T_1 increases monotonically with temperature, and T_1 was continuous at the phase transition temperatures. However, the T_1 undergoes a change in slope near T_{C4}. ^{1}H T_1 passes through a minimum value in the vicinity of 220 K, and the presence of this minimum was attributed to the effects of molecular motion. The relaxation process from the ^{1}H T_1 curve was affected by molecular motion, as described by the BPP theory.[33] The activation energy in the low and high temperatures was reported 29.95 ± 0.85 kJ mol^{-1} and 10.99 ± 0.37 kJ mol^{-1}, respectively.

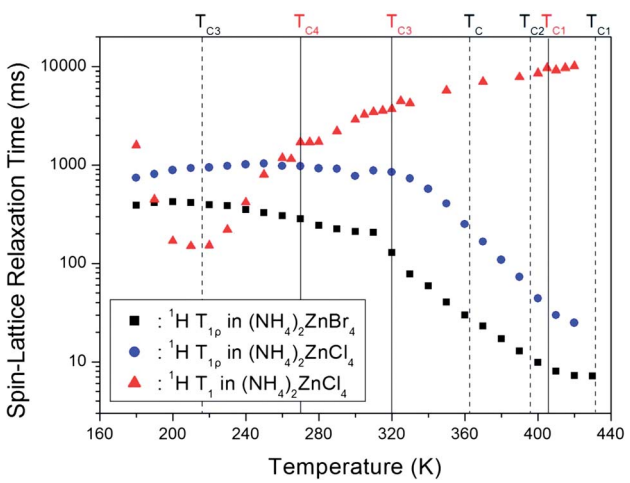

Fig. 5 Temperature dependences of the spin-lattice relaxation time, $T_{1\rho}$, in the rotating frame and the spin-lattice relaxation time, T_1, in the laboratory frame of the ^{1}H nuclei in $(NH_4)_2ZnCl_4$ and $(NH_4)_2ZnBr_4$ ($(NH_4)_2ZnCl_4$: solid lines, $(NH_4)_2ZnBr_4$: dash lines).

3.3 Structural changes near phase transition temperatures from ^{14}N NMR

In order to investigate local phenomena related to successive phase transitions, the NMR spectra of ^{14}N ($I = 1$) was obtained as a function of temperature using static NMR at a Larmor frequency of $\omega_0/2\pi = 43.342$ MHz. ^{14}N ($I = 1$) NMR is a sensitive method for probing local structural properties in each phase. The ^{14}N NMR spectra consisted of pairs of lines at frequencies corresponding to the transitions $\Delta m = \pm 1 \leftrightarrow \Delta m = 0$. The crystal was oriented such that the magnetic field was aligned with the crystallographic c-axis. Temperature-dependent changes in the ^{14}N resonance frequency are generally attributed to changes in the structural geometry, indicating a change in the quadrupole coupling constant of the ^{14}N nuclei. The ^{14}N NMR spectra at phase I, II, III, IV, and VI in $(NH_4)_2ZnCl_4$ crystals were plotted in Fig. 6. Here, the ^{14}N peaks positions were denoted by close circles. Two resonance lines were expected because of the quadrupole interaction of the ^{14}N nucleus. However, many resonance lines were observed, and they were much narrower in line width.

The resonance frequencies of ^{14}N signals in $(NH_4)_2ZnCl_4$ and $(NH_4)_2ZnBr_4$ single crystals are respectively plotted in Fig. 7(a) and (b) as a function of temperature. In the case of $(NH_4)_2ZnCl_4$, the phase transitions occurring at T_{C1}, T_{C3}, and T_{C4} were observed from our DSC results, whereas those at T_{C2} and T_{C5} were not observed. Therefore, T_{C1}, T_{C3}, and T_{C4} are denoted by solid lines, and T_{C2} and T_{C5} are denoted dotted lines in Fig. 7(a).

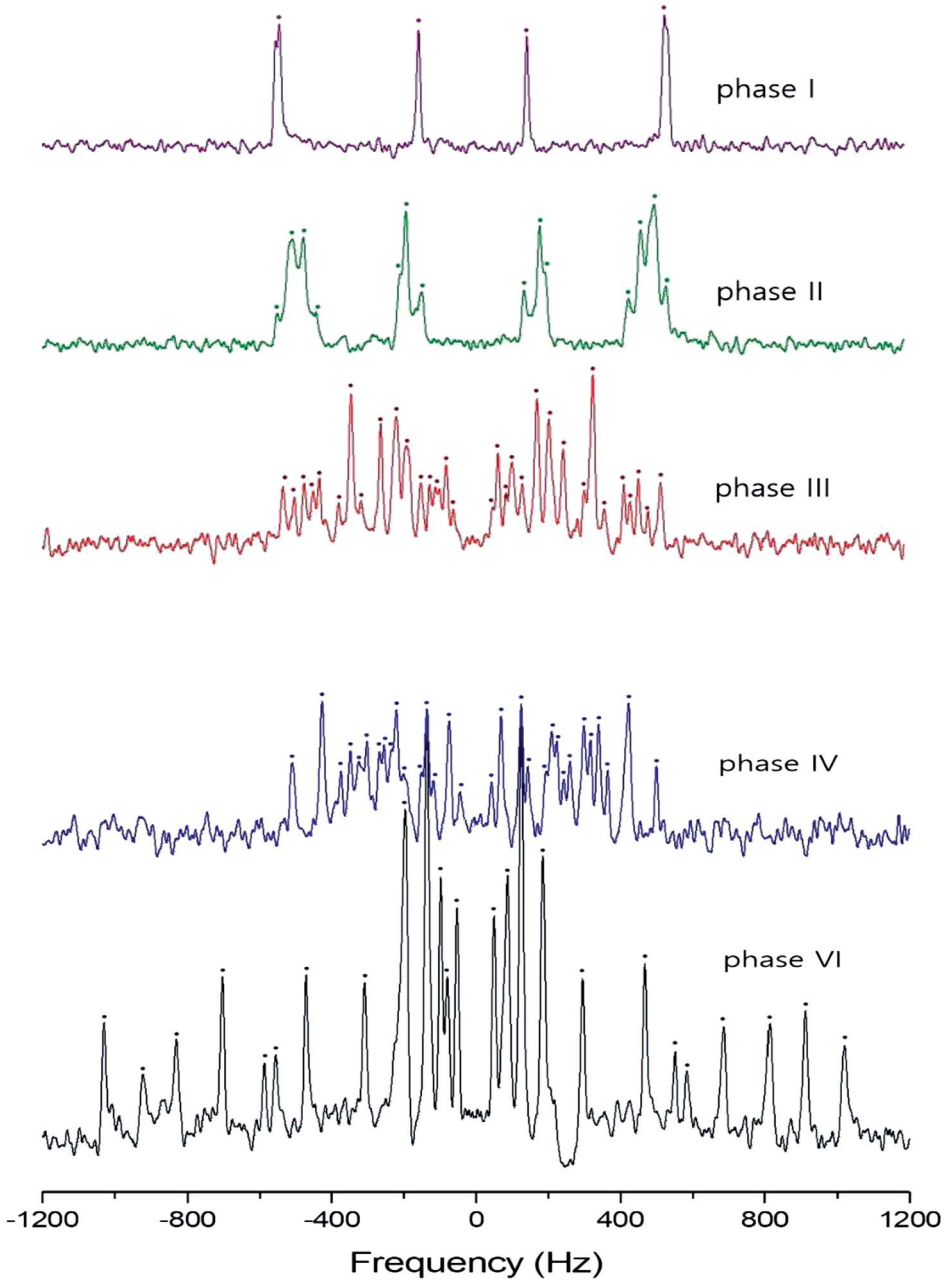

Fig. 6 ^{14}N NMR spectra in $(NH_4)_2ZnCl_4$ single crystal at phase I, II, III, IV, and VI.

The resonance frequencies near T_{C1}, T_{C4}, and T_{C5} changed, whereas those near T_{C2} and T_{C3} did not change. In phase I, each unit cell contains four formula units, and there are also two different kinds of ^{14}N nuclei, termed N(1) and N(2). Therefore, the ^{14}N NMR spectra exhibited eight resonance lines in four pairs. Here, the two inequivalent sites N(1) and N(2) are distinguished by the quadrupole coupling constant previously reported: $e^2qQ/h = 105.5$ kHz and $\eta = 0.96$ for N(1), and $e^2qQ/h = 48.2$ kHz and $\eta = 0.087$ for N(2).[27] Additional lines in phases II, III, and IV were obtained, although they exhibited very small intensities compared with phase I. In phases III and IV, the unit cell is quadrupoled along the *c*-direction of phase I. The unit cell of phases III and IV contains 16 formula units, and thus 32 resonance lines of 16 pairs are expected. According to the crystallography results shown in Fig. 1(b), eight atoms N(11), N(21), N(31), and N(41) are surrounded by five Cl atoms, while the other atoms N(12), N(22), N(32), and N(42), which are located between the layers created by the $ZnCl_4$ tetrahedra, are surrounded by eight Cl atoms. From the NMR spectra results of 16 pairs of ^{14}N, the approximately 32 resonance lines in phases III and IV were measured, as shown in Fig. 7(a). The 32 resonance lines from the 16 pairs of ^{14}N in the NH_4 ion were consistent with the previously reported crystallography structure.[12,16,17] In addition, phase VI, below T_{C5}, contains $Z = 12$ formula units, N(11), N(12), N(21), N(22), N(31), and N(32), as shown in Fig. 1(c). Therefore, approximately 24 resonance lines

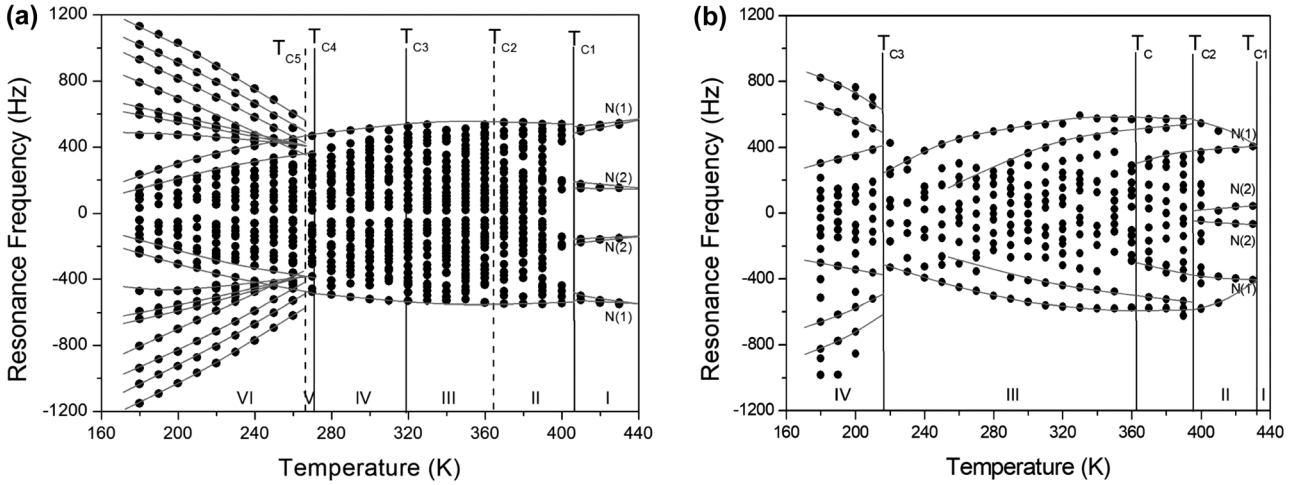

Fig. 7 (a) Resonance frequency of ^{14}N NMR spectra in $(NH_4)_2ZnCl_4$ single crystal as a function of temperature. (b) Resonance frequency of ^{14}N NMR spectra in $(NH_4)_2ZnBr_4$ single crystal as a function of temperature.

in 12 pairs were obtained. In these results, the splitting of the ^{14}N resonance lines for seven of the pairs slightly decreased with increasing temperature, whereas those of the ^{14}N resonance lines for the other five pairs slightly increased with increasing temperature. On the other hand, the resonance frequencies in phases I, II, III, and IV for the case of $(NH_4)_2ZnBr_4$ are shown in Fig. 7(b). The ^{14}N NMR spectra from $(NH_4)_2ZnBr_4$ could not be easily observed in detail because of their very low intensity. However, the resonance frequencies near T_{C2} and T_{C3} changed discontinuously.

As mentioned above, in the case of $(NH_4)_2ZnCl_4$, four pairs of lines ascribed to N(1) and N(2) nuclei appeared in phase I, above 406 K. Because the frequency distributions in phase II discontinuously emerged from these high-temperature lines, the notations N(1) and N(2) were not retained. Based on this temperature dependence, the assignment of the resonance lines in phases III and IV are also not denoted. The resonance frequency from phase V cannot be distinguished because of the much narrower temperature range. The resonance frequencies in phase VI, below T_{C4}, changed discontinuously from those of phases V and IV. The changes in the resonance lines near T_{C4} for $(NH_4)_2ZnCl_4$ and T_{C3} for $(NH_4)_2ZnBr_4$ also indicated a phase transition where the new phase exhibited orthorhombic symmetry, which equates to a higher degree of symmetry compared with monoclinic symmetry. Abrupt changes in the resonance frequencies for ^{14}N near the phase transition temperatures are generally attributed to structural phase transitions.

4. Conclusion

Data on structural geometries near successive phase transition temperatures of $(NH_4)_2ZnX_4$ (X = Cl, Br) were obtained by ^1H MAS NMR and ^{14}N NMR as a function of temperature. We studied the molecular motions in $(NH_4)_2ZnX_4$, based on the ^1H chemical shifts and spin-lattice relaxation time, $T_{1\rho}$, in the rotating frame. The ^1H chemical shifts near the phase transition temperatures for the two materials did not show any drastic change, and this result might be related to proton ordering near the phase transition temperatures. From the ^1H $T_{1\rho}$ results, the activation energies for the tumbling motion of ^1H had very similar values, and the tumbling motion of NH_4^+ ions occurred within the high-temperature range.

We compared the ^1H MAS NMR in the rotating frame measured here and the previously reported ^1H static NMR results in the laboratory frame[23–25] for $(NH_4)_2ZnCl_4$. The trends in $T_{1\rho}$ values for ^1H in $(NH_4)_2ZnCl_4$ are different from the trends in the T_1 values. The molecular motion by $T_{1\rho}$ in the rotating frame was dominant at high temperature, whereas that by T_1 in the laboratory frame was dominant at low temperature. The activation energy values extracted from $T_{1\rho}$ and T_1 measurements are different for the molecular motions in the kHz and MHz ranges.

The ^{14}N NMR spectra exhibited a sudden shift in the ^{14}N peak positions and number of peaks at the phase transition temperatures. The electric field gradient (EFG) tensors at the N sites varied, reflecting the changing atomic configurations around the ^{14}N nuclei. This is because the phase transition temperature strongly affect the ^{14}N number of symmetry related nitrogen centers within the unit cell. Therefore, ^{14}N NMR provides insight into changes in crystal symmetry and cation reorientation rates induced by heating and phase transitions.

The two crystals have different phase transition temperatures, but seemingly similar phase transition mechanisms. Although $(NH_4)_2ZnX_4$ has different bond lengths in the Zn–X (X = Cl, Br) structure, and different X atomic radii, the different halide ions (X = Cl, Br) do not appear to significantly influence the ^1H relaxation time.

Conflicts of interest

There are no conflicts to declare.

Acknowledgements

This research was supported by the Basic Science Research Program through the National Research Foundation of Korea (NRF), funded by the Ministry of Education, Science, and Technology (2016R1A6A1A03012069 and 2015R1A1A3A04001077).

References

1 C. Griset, S. Head, J. Alices and O. A. Starykh, *Phys. Rev. B*, 2011, **84**, 245108.
2 T. Ono, H. Tanaka, Y. Shirata, A. Kindo, F. Ishikawa, O. Kolomiyets, H. Mitamura, T. Goto, N. Nakano, N. A. Fortune, S. T. Hannahs, Y. Yoshida and Y. Takano, *J. Phys.: Conf. Ser.*, 2011, **302**, 12003.
3 M. Vachon, G. Koutroulakis, V. F. Mitrovic, O. Ma, J. B. Marston, A. P. Reyes, P. Kuhns, R. Coldea and Z. Tylczynski, *New J. Phys.*, 2011, **13**, 93029.
4 K. Foyevtsova, I. Opahle, Y.-Z. Ahang, H. O. Jeschke and R. Valenti, *Phys. Rev. B*, 2011, **83**, 125126.
5 T. Coletta, M. E. Zhitomirsky and F. Mila, *Phys. Rev. B*, 2013, **87**, 60407.
6 S. A. Zvyagin, D. Kamenskyi, M. Ozerov, J. Wosnitza, M. Ikeda, T. Fujita, M. Hagiwara, A. I. Smirnov, T. A. Soldatov, A. Ya Shapiro, J. Krzystek, R. Hu, H. Ryu, C. Petrovic and M. E. Zhitomirsky, *Phys. Rev. B*, 2014, **112**, 77206.
7 A. Yamada, *Phys. Rev. B*, 2014, **90**, 235138.
8 J. Merino, *Phys. Rev. B*, 2014, **89**, 245112.
9 S. A. Zvyagin, M. Ozerov, D. Kamenskyi, J. Wosnitza, J. Krzystek, D. Yoshizawa, W. Hagiwara, R. Hu, H. Ryu, C. Petrovic and M. E. Zhitomirsky, *New J. Phys.*, 2015, **17**, 113059.
10 B. Schmidt and P. Thalmeier, *New J. Phys.*, 2015, **17**, 73025.
11 D. J. Kubicki, D. Prochowicz, A. Hofstetter, P. Pechy, S. M. Zakeeruddin, M. Gratzel and L. Emsley, *J. Am. Chem. Soc.*, 2017, **139**, 10055.
12 H. Matsunaga, *J. Phys. Soc. Jpn.*, 1982, **51**, 864.
13 H. Matsunaga and E. Nakamura, *J. Phys. Soc. Jpn.*, 1981, **50**, 2789.
14 T. Sata, T. Osaka and Y. Makita, *J. Phys. Soc. Jpn.*, 1984, **53**, 1907.
15 A. K. Moskalev, I. A. Belobrova, L. I. Zherebtsova and I. P. Aleksandrova, *Phys. Status Solidi A*, 1982, **72**, k19.
16 I. Mikhail, *Acta Crystallogr., Sect. B: Struct. Crystallogr. Cryst. Chem.*, 1980, **36**, 2126.
17 H. Matsunaga, K. Ithoh and E. Nakamura, *Acta Crystallogr., Sect. B: Struct. Crystallogr. Cryst. Chem.*, 1982, **38**, 898.
18 T. Osaka, M. Komukae and Y. Makita, *J. Phys. Soc. Jpn.*, 1982, **51**, 3409.
19 H. V. Koningsveld, *Acta Crystallogr., Sect. C: Cryst. Struct. Commun.*, 1983, **39**, 15.
20 T. Sato, T. Osaka and Y. Makita, *J. Phys. Soc. Jpn.*, 1983, **52**, 3297.
21 W. J. Asker, D. E. Scaife and J. A. Watts, *Aust. J. Chem.*, 1972, **25**, 2301.
22 H. Shigematsu, H. Kasano and H. Mashiyama, *J. Phys. Soc. Jpn.*, 1993, **62**, 3929.
23 A. R. Lim, *Solid State Commun.*, 2011, **151**, 1631.
24 A. R. Lim and K.-Y. Lim, *J. Solid State Chem.*, 2013, **200**, 227.
25 A. R. Lim, *Chem. Phys.*, 2012, **400**, 39.
26 K. P. Ramesh, N. Devaraj, D. Vijayaraghavan and J. Ramakrishna, *Phase Transitions*, 1992, **37**, 203.
27 D. Michel, B. Muller, J. Petersson, A. Trampert and R. Walisch, *Phys. Rev. B*, 1991, **43**, 7507.
28 J. L. Koenig, *Spectroscopy of Polymers*, Elsevier, New York, 1999.
29 Z. Tylczynski and P. Piskunowicz, *Phys. Status Solidi A*, 1990, **118**, 441.
30 J. P. Strivastava and A. Kulshreshtha, *J. Opt. Soc. Am. B*, 1991, **8**, 2379.
31 A. Agarwal, M. B. Patel, M. Pal and H. D. Bist, *Spectrochim. Acta, Part A*, 1984, **40**, 1063.
32 A. M. Gillet, Y. Luspin and G. Hauret, *Solid State Commun.*, 1987, **64**, 797.
33 N. Bloembergen, E. M. Purcell and R. V. Pound, *Phys. Rev.*, 1948, **73**, 679.
34 A. R. Lim, *AIP Adv.*, 2016, **6**, 35307.
35 A. Abragam, *The Principles of Nuclear Magnetism*, Oxford University Press, 1961.